

# Distributed Motion Control of Multiple Mobile Manipulators for Reducing Interaction Wrench in Object Manipulation

Wenhang Liu, Meng Ren, Kun Song, Gaoming Chen, Michael Yu Wang, *Fellow, IEEE*, and Zhenhua Xiong, *Member, IEEE*

**Abstract**—In real-world cooperative manipulation of objects, multiple mobile manipulator systems may suffer from disturbances and asynchrony, leading to excessive interaction wrenches and potentially causing object damage or emergency stops. This paper presents a novel distributed motion control approach aimed at reducing these unnecessary interaction wrenches. The control strategy for each robot only utilizes information from the local force sensors and neighboring robots, without the need for global position and velocity information. Disturbances are corrected through compensatory movements of the manipulators. Besides, the robustness of the control law against communication delays between robots is also considered. The stability of the control law is rigorously proven by the Lyapunov theorem. Subsequently, the efficacy of the proposed control law is validated through simulations and experiments of collaborative object manipulation by two robots. Experimental results demonstrate the effectiveness of the proposed control law in reducing interaction wrenches during object manipulation.

**Note to Practitioners**—This work is motivated by reducing the interaction wrenches in the cooperative manipulation of objects by multiple mobile manipulator robots. During manipulation, robots often grip the object tightly, and any disturbance in the motions can result in increased interaction wrenches. These interaction wrenches do not contribute to supporting or manipulating the object but may damage both the object and the robots. Previous methods typically rely on extensive global position and velocity information or torque control of robots, which are not common in industrial settings and robots. Thus, their methods are challenging to validate or apply practically. This work introduces a novel distributed control law for reducing interaction wrenches, which only requires information from the local force sensors and neighboring robots. Moreover, the robustness of the control law against communication delays is considered. The proposed control law is convenient to apply and has been verified in physical robots, demonstrating its practical applicability.

**Index Terms**—Multiple mobile manipulator system, object manipulation, distributed control, interaction wrench.

This work was supported in part by the National Natural Science Foundation of China (U1813224) and MoE Key Lab of Artificial Intelligence, AI Institute, Shanghai Jiao Tong University, China. (*Corresponding author: Zhenhua Xiong.*)

Wenhang Liu, Meng Ren, Kun Song, Gaoming Chen, and Zhenhua Xiong are with the School of Mechanical Engineering, State Key Laboratory of Mechanical System and Vibration, Shanghai Jiao Tong University, Shanghai, China (e-mail: liuwenhang@sjtu.edu.cn; meng\_ren@sjtu.edu.cn; coldtea@sjtu.edu.cn; cgm1015@sjtu.edu.cn; mexiong@sjtu.edu.cn).

Michael Yu Wang is with the School of Advanced Engineering, Great Bay University, Guangdong, China, and also with the Department of Mechanical and Aerospace Engineering, Hong Kong University of Science and Technology, Clear Water Bay, Hong Kong (e-mail: mywang@gbu.edu.cn; mywang@ust.hk).

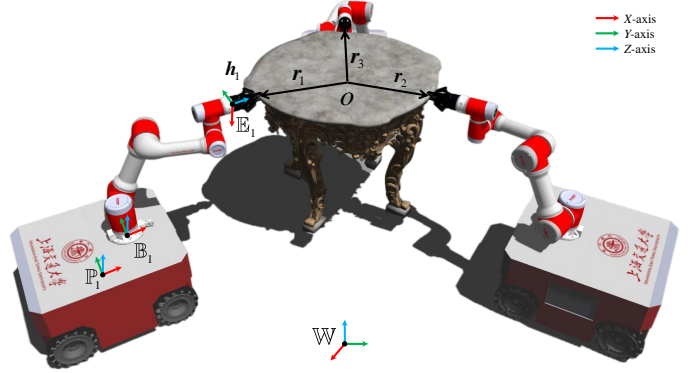


Fig. 1. Three mobile manipulator robots collaboratively manipulate an object. Some basic coordinate frames are labeled.

## I. INTRODUCTION

**M**OBILE manipulator robots combine the extensive mobility of a mobile platform with the dexterous manipulation capabilities of a robotic manipulator. This integration allows them to be used in various industrial applications, including object delivery, assembly, machining, and transportation [1]–[3]. As the complexity of industrial tasks rises, the limitations of single robots become apparent. Tasks such as manipulating large objects and performing complex assemblies often require the collaboration of multiple robots [4] [5]. Moreover, multi-robot collaboration offers more advantages, such as efficiency, robustness, adaptivity, and flexibility [6]. Therefore, in industrial automation, Multiple Mobile Manipulator Systems (MMMS) have attracted widespread attention in object manipulation. A case is shown in Fig. 1. In MMMS collaboration, establishing desired consistency or formations is crucial, such as coordinated formations, motions, and wrenches. In related research, some studies focus on motion planning problems, mainly including redundant and coordinated planning [7].

However, when executing these planned trajectories in real-world scenarios, achieving perfect consistency becomes impossible due to numerous factors such as interactions with objects and some uncertainties. Due to the tight coupling between robots and the object, even small disturbances may cause excessive interaction wrenches. These unnecessary interaction wrenches do not contribute to supporting the object, instead, they may lead to emergency stops of robots or damage

to the object [8] [9]. While attentive planning is essential for guiding the robots, robust control strategies that can adapt to uncertainties are equally or even more crucial for achieving reliable performance in practical applications [10].

Cooperative control of MMMS in object manipulation, therefore, is an essential area of research. Based on adaptive impedance control and the leader-follower method, the prescribed performance of MMMS in object transportation was achieved in [11]. To track the reference trajectory and avoid obstacles, a method integrating formation control with constrained optimization for MMMS was proposed in [12]. The constrained optimization was solved by a discontinuous projected primal-dual algorithm with damping terms. A constrained optimization method for multi-robot formation control in dynamic environments was proposed in [13], optimizing formation parameters to avoid collisions and progress toward goals. The approach included local motion planning via sequential convex programming and global path planning through sampling and graph search. The above studies enable MMMS to achieve some desired coordination performance.

Generally, the control strategies of MMMS can be categorized into centralized, leader-follower, and fully distributed methods. Centralized methods employ a central controller to control the movements and motions of all mobile manipulators [14]. These methods benefit from a global perspective, enabling optimal task allocation and coordination strategies. However, centralized methods suffer from scalability issues as the number of robots increases [15]. The computational burden on the central controller grows, and the system becomes vulnerable to a single point of failure. In recent years, more attention has been given to the latter two methods in research.

The leader-follower method simplifies the coordination problem by designating one or more robots as the leaders and the others as followers. The leaders make the primary decisions, and the followers adjust their motions based on the leaders' state to reduce unnecessary interaction wrenches. In [16], a leader-follower structure was used for MMMS to cooperatively transport objects in a constrained workspace. It combined novel estimation laws and adaptive control to enhance robust motion control and collision avoidance. Leader-follower control of MMMS for collective object transportation was investigated in [17], optimizing for energy efficiency and manipulability. The stability of the closed-loop system was proven, and simulations demonstrated the effectiveness of this optimization scheme. In [18], the control algorithm simulated impedance dynamics at each manipulator's grasping point, enabling coordinated handling based on a leader-follower approach. In [19] and [20], every follower synchronized to the direction of the force applied by one leader robot through the unified or proportional force-amplifying framework. The leader-follower method was validated in physical experiments in [18]–[20]. It reduces the complexity of control for the followers and is easier to implement on real-world robots. However, the system's overall performance heavily relies on the leader's reliability and decision-making capabilities, introducing a potential single point of failure similar to centralized methods.

Fully distributed methods represent the most advanced ap-

proach, emphasizing decentralized control where each mobile manipulator makes decisions based on local information and communication with neighboring robots. In [21], a distributed adaptive controller was proposed to achieve synchronization based on the desired load distribution and desired internal force. The effectiveness of their method was validated through experiments. A distributed model predictive control method was presented for MMMS to transport objects with respect to state, control input, and synchronization constraints in [22]. The method simplifies the problem into two independent synchronization tracking control issues for task-space end-effectors and null-space mobile bases. In [23], a chatterless integral sliding mode force-position control was proposed. Each robot was designed to correct collectively the velocity deviation due to the pushing of the other robots. Distributed coordination and cooperation control for networked mobile manipulators over a topology was introduced in [24]. Synchronization control combined with force controls ensured cooperative manipulation and transportation. In [25], a control approach was proposed to guarantee predefined transient and steady-state performance for object trajectory. Load distribution between robots was also considered by using a grasp matrix pseudoinverse.

While fully distributed methods have significantly advanced the control and coordination of multiple mobile manipulators, they exhibit certain limitations when applied to real-world scenarios. First, existing methods often depend on accurate global positions or velocities of all robots to achieve effective coordination [12], [21], [23]–[26]. In industrial automation environments, obtaining precise global positioning can be very challenging. The reliance on global data makes these control methods less robust and difficult to apply. Second, many of these approaches require torque control of the robots [21], [22], [24], [25], [27]. Torque control demands sophisticated hardware and software capabilities, including high-fidelity sensors which may not be present in all industrial robots. This limitation restricts the applicability of these methods to only those systems that are specifically designed and equipped for torque control. Third, distributed methods often require communication between robots to share local information and maintain coordination. In practice, communication delays are inevitable. The aforementioned methods have not been validated for robustness against such delays.

Therefore, to address these shortcomings and make MMMS more convenient and applicable in real-world object manipulation, this paper presents a distributed motion control strategy. The strategy aims to reduce unnecessary interaction wrenches and does not rely on global position, velocity data, or torque control. Instead, each robot leverages information from the local force sensor and other robots to achieve disturbance correction through manipulator motions, addressing uncertainties such as kinematic inaccuracies. The stability of the proposed control law is demonstrated through the Lyapunov theorem. Additionally, the study explores the relationship between delay limits, control parameters, and object stiffness. Finally, the control law is validated through simulations and physical experiments. Both results show that the method can effectively reduce interaction wrenches.

The main contributions of this paper are twofold. First, the proposed distributed motion control law utilizes local force sensors and inter-robot communication to reduce interaction wrenches without requiring extensive global data or torque control. In contrast, existing methods often rely on these, which can be challenging to obtain in industrial settings. Second, the stability of the proposed control law against communication delays is rigorously proven using the Lyapunov theorem, ensuring robust performance. Then, the control law is implemented on physical robots and the results demonstrate the effectiveness in reducing interaction wrenches.

The remainder of this paper is organized as follows. In Section II, some basic concepts are defined. In Section III, the problem is formulated and the proposed control law is presented. Also, the method is proven theoretically and verified by simulations. In Section IV, experiments are conducted on physical robots and results are analyzed. Finally, Section V concludes the paper and outlines future work.

## II. PRELIMINARIES

### A. Kinematics of Mobile Manipulator

A mobile manipulator robot usually consists of a mobile platform and a mounted robotic manipulator. This paper considers an omnidirectional mobile platform and a six-degree-of-freedom manipulator. As shown in Fig. 1, three mobile manipulators cooperatively manipulate objects.  $\mathbb{W}$  denotes the frame of the world.  $\mathbb{P}_i$ ,  $\mathbb{B}_i$ , and  $\mathbb{E}_i$  denote the frames of the mobile platform, the base of the manipulator, and the end-effector of the  $i$ -th mobile manipulator, respectively,  $i = 1, \dots, n$ . Let  $\mathbf{T}$ ,  $\mathbf{R}$ ,  $\mathbf{P}$  represent the relationship between different frames. For example,  ${}^{\mathbb{W}}_{\mathbb{E}_i}\mathbf{T} \in SE(3)$  represents the pose of frame  $\mathbb{E}_i$  in frame  $\mathbb{W}$ ,  ${}^{\mathbb{W}}_{\mathbb{E}_i}\mathbf{R} \in SO(3)$  represents the orientation of frame  $\mathbb{E}_i$  in frame  $\mathbb{W}$ , and  ${}^{\mathbb{W}}_{\mathbb{E}_i}\mathbf{P} \in \mathbb{R}^3$  represents the translation of frame  $\mathbb{E}_i$  in frame  $\mathbb{W}$ . The forward kinematics of the robot is

$$\mathbf{e}_i = f_{\text{mm}}(\mathbf{q}_{\text{mm},i}) \quad (1)$$

where  $\mathbf{e}_i \in \mathbb{R}^6$  is the pose of the end-effector in frame  $\mathbb{W}$ ,  $f_{\text{mm}}(\cdot)$  is related to  ${}^{\mathbb{W}}_{\mathbb{E}_i}\mathbf{T}$ , and  $\mathbf{q}_{\text{mm},i} \in \mathbb{R}^9$  is the configuration of the robot. Specifically,  $\mathbf{q}_{\text{mm},i} = [\mathbf{q}_{\text{p},i}^{\text{T}}, \mathbf{q}_i^{\text{T}}]^{\text{T}}$ , where  $\mathbf{q}_{\text{p},i} \in \mathbb{R}^3$  is the configuration the mobile platform and  $\mathbf{q}_i \in \mathbb{R}^6$  is the configuration the manipulator. Differentiating Eq.(1), the velocity relationship is

$$\dot{\mathbf{e}}_i = \mathbf{J}_{\text{mm},i}(\mathbf{q}_{\text{mm},i})\dot{\mathbf{q}}_{\text{mm},i} \quad (2)$$

where  $\mathbf{J}_{\text{mm},i} = [\mathbf{J}_{\text{p},i}, \mathbf{J}_i]^{\text{T}}$  is the Jacobian matrix of the robot.

### B. Force Sensor

In order to manipulate objects, the end of the manipulator is usually equipped with a gripper and a force sensor. The data measured by force sensors are usually in their own coordinate systems. Let  ${}^{\mathbb{E}_i}\mathbf{h}_i = [{}^{\mathbb{E}_i}\mathbf{f}_i^{\text{T}}, {}^{\mathbb{E}_i}\mathbf{t}_i^{\text{T}}]^{\text{T}}$  represent the data measured by the sensor at the end effector of the  $i$ -th robot.  $\mathbf{h}_i = [\mathbf{f}_i^{\text{T}}, \mathbf{t}_i^{\text{T}}]^{\text{T}}$  represents the force and torque exerted on the end of the  $i$ -th robot in frame  $\mathbb{W}$ . According to the force transfer relationship, it can be derived

$$\mathbf{f}_i = {}^{\mathbb{W}}_{\mathbb{E}_i}\mathbf{R} \cdot {}^{\mathbb{E}_i}\mathbf{f}_i \quad \mathbf{t}_i = {}^{\mathbb{W}}_{\mathbb{E}_i}\mathbf{R} \cdot {}^{\mathbb{E}_i}\mathbf{t}_i \quad (3)$$

Before measuring force data, it is necessary to perform calibration and gravity compensation for the force sensor. In unloaded conditions, the force data consists of

$${}^{\mathbb{E}_i}\mathbf{h}_i = \begin{bmatrix} {}^{\mathbb{E}_i}\mathbf{f}_i \\ {}^{\mathbb{E}_i}\mathbf{t}_i \end{bmatrix} = \begin{bmatrix} \mathbf{f}_{\text{s},0} \\ \mathbf{t}_{\text{s},0} \end{bmatrix} + \begin{bmatrix} \mathbf{f}_{\text{s},g} \\ \mathbf{t}_{\text{s},g} \end{bmatrix} \quad (4)$$

where  $\mathbf{f}_{\text{s},0}$  and  $\mathbf{t}_{\text{s},0}$  are the drift errors,  $\mathbf{f}_{\text{s},g}$  and  $\mathbf{t}_{\text{s},g}$  are caused by the gravity of the gripper  $mg$ . The displacement from the sensor to the gripper's center of mass is denoted as  ${}^{\mathbb{E}_i}_{g}\mathbf{P}$ . Parameters  $\mathbf{f}_{\text{s},0}$ ,  $\mathbf{t}_{\text{s},0}$ ,  ${}^{\mathbb{E}_i}_{g}\mathbf{P}$ , and  $mg$ , which need further calibration, are linearly independent. Therefore, these parameters can be calculated using the least squares method after obtaining enough sensor data in unloaded conditions [28].

The total wrench applied to the object by robots is

$$\mathbf{h}_o = -\mathbf{G} [\mathbf{h}_1^{\text{T}} \quad \dots \quad \mathbf{h}_n^{\text{T}}]^{\text{T}} \quad (5)$$

where  $\mathbf{G}_{6 \times 6n}$  is the grasp matrix, which is only related to the relative poses of the grasping points and the object's center of mass [21], [29], [30], as the  $\mathbf{r}_1, \mathbf{r}_2, \mathbf{r}_3$  shown in Fig. 1.

### C. Graph Theory

The communication structure of a system with  $n$  robots can be typically represented on graphs. Let  $\mathcal{G} = (\mathcal{V}, \mathcal{E})$  denote a graph, where  $\mathcal{V} = \{v_i\}$  is the vertex set and  $\mathcal{E} = \{a_{ij}\}$  is the edge set.  $a_{ij} = 1$  if the  $i$ -th robot can received information from the  $j$ -th robot, otherwise  $a_{ij} = 0$ . The adjacency matrix of the graph is  $\mathbf{A} = (a_{ij}) \in \mathbb{R}^{n \times n}$ . The degree matrix of the graph is  $\mathbf{D} = \text{diag} \left\{ \sum_{j=1}^n a_{ij} \right\} \in \mathbb{R}^{n \times n}$ . The Laplacian matrix of the graph is  $\mathbf{L} = \mathbf{D} - \mathbf{A}$ . In this paper, the directed graph is considered, which denotes  $a_{ij} \neq a_{ji}$ .

## III. THE PROPOSED CONTROL METHOD

### A. Problem Statement and Control Law

*Assumption 1:* The robot grasps the object tightly with its gripper, ensuring no slippage and sufficient force transmission during motion.

*Assumption 2:* Each robot receives information from at least one other robot, which is  $\sum_{j=1}^n a_{ij} \geq 1$ . The upper bound for communication delay between robots is  $\tau$ .

*Assumption 3:* The motion of robots in cooperative object manipulation is a quasi-static process.

*Assumption 1* is a very general assumption, which can also be found in [11], [21], [31]–[33]. Other assumptions are further discussed in subsequent theoretical proofs and experiments.

For the planning of cooperative manipulation of objects by multiple mobile manipulator robots, there are several references. This paper considers the motion control problem of executing a planned cooperative manipulation trajectory. For the sake of brevity,  $\mathbf{q}(t)$  is abbreviated as  $\mathbf{q}$  in the absence of time delay. For each robot, assuming that  $\mathbf{h}_i^{\text{ref}}$ ,  $\dot{\mathbf{h}}_i^{\text{ref}}$ ,  $\mathbf{q}_{\text{mm},i}^{\text{ref}}$ , and  $\dot{\mathbf{q}}_{\text{mm},i}^{\text{ref}}$  have been planned. Since the manipulation is a quasi-static process, the desired wrench of the object  $\mathbf{h}_o^d$  equals the gravity of the object. Then,  $\mathbf{h}_i^{\text{ref}}$  and  $\dot{\mathbf{h}}_i^{\text{ref}}$  can be calculated by

$$[\mathbf{h}_1^{\text{T}} \quad \dots \quad \mathbf{h}_n^{\text{T}}]^{\text{T}} = -\mathbf{G}^{\dagger} \mathbf{h}_o^d \quad (6)$$

where  $\mathbf{G}^\dagger$  is the generalized inverse of  $\mathbf{G}$ . The load distribution  $\mathbf{h}_i^{\text{ref}}$  is achieved based on the specific form of  $\mathbf{G}^\dagger$  [30]. The motions are planned according to the desired trajectory of the object.

The desired trajectories and interaction wrenches are achieved if  $\mathbf{q}_{\text{mm},i}^{\text{ref}}$  is the input. However, due to model deviations and disturbances, this ideal situation is almost impossible. If global positioning and velocity information could be obtained, the correction process would be relatively easy since the actual velocity is corrected to match the desired velocity. However, this often requires high-precision and large-scale positioning systems, which are often difficult to implement [26]. Therefore, information from local force sensors is considered to design the control laws. Besides, it is also important to consider the communication delay between robots as it is a very common situation in reality. Let  $\tau_{ij}(t)$  denote the time delay in the  $i$ -th robot receiving information from the  $j$ -th robot. In this paper, the most general delays are considered. The communication delays are non-uniform, asymmetric, time-varying, and unknown. For example,  $\tau_{12}(t) \neq \tau_{21}(t)$ ,  $\tau_{12}(t) \neq \tau_{13}(t)$ , and thus robots cannot achieve synchronization by querying their own historical information when receiving unknown communication delays.

Since the object is not an absolute rigid body, the actual force exerted on the  $i$ -th robot during motion by the object is

$$\begin{aligned} \mathbf{h}_i - \mathbf{h}_i^{\text{ref}} &= K \left( \sum_{j=1, j \neq i}^n (\Delta \mathbf{e}_j - \Delta \mathbf{e}_i) \right) \\ \Delta \mathbf{e}_i &= \mathbf{e}_i - \mathbf{e}_i^{\text{ref}} \end{aligned} \quad (7)$$

where  $K_{6 \times 6} > 0$  is a diagonal matrix, representing the stiffness in six dimensions of the object. Eq.(7) can be rewritten as

$$\mathbf{h}_i - \mathbf{h}_i^{\text{ref}} = K(\mathbf{e}_i^{\text{d}} - \mathbf{e}_i) \quad (8)$$

where  $\mathbf{e}_i^{\text{d}}$  is the desired correction target. Through the force sensor, the direction of correction can be obtained.

It is well known that the manipulator is more accurate and controllable than the mobile platform [34]. In general, deviations in the executed planned trajectory are relatively small and can be corrected within the workspace of the manipulator. Therefore, the desired correction target is achieved through the manipulator. The control law of the manipulator for maintaining desired interaction wrenches is as follows

$$\begin{aligned} \mathbf{u}_i &= -k \sum_{j=1}^n a_{ij} \left[ f^{-1}(K_0^{-1}(\mathbf{h}_i^{\text{ref}} - \mathbf{h}_i)) \right. \\ &\quad \left. - \beta f^{-1}(K_0^{-1}(\mathbf{h}_j^{\text{ref}}(t - \tau_{ij}) - \mathbf{h}_j(t - \tau_{ij}))) \right] \end{aligned} \quad (9)$$

where  $k$  and  $\beta$  are positive coefficients,  $K_0$  is an estimate or empirical value of the stiffness, and  $f^{-1}(\cdot)$  is the inverse kinematics of the manipulator. The input required for this control law is the local force sensor information, current joint position of the manipulator, and the information from neighboring robots. The control law ensures that the end of the robot moves towards the desired target  $\mathbf{e}_i \rightarrow \mathbf{e}_i^{\text{d}}$ , thereby maintaining the interaction wrench at the expected value  $\mathbf{h}_i \rightarrow \mathbf{h}_i^{\text{ref}}$ .

Eq.(8) can be rewritten in the joint space as

$$\mathbf{h}_i - \mathbf{h}_i^{\text{ref}} = K(f(\mathbf{q}_i^{\text{d}}) - f(\mathbf{q}_i)) \quad (10)$$

where  $\mathbf{q}_i^{\text{d}}$  is the desired correction joint target. Substituting Eq.(10) into Eq.(9) and let  $\kappa = kK_0^{-1}K$ , the control law can be rewritten as

$$\mathbf{u}_i = -\kappa \sum_{j=1}^n a_{ij} ((\mathbf{q}_i - \mathbf{q}_i^{\text{d}}) - \beta(\mathbf{q}_j(t - \tau_{ij}) - \mathbf{q}_j^{\text{d}}(t - \tau_{ij}))) \quad (11)$$

Eq.(9) is the control law used in actual calculations, indicating the input and output. The control rate is written as Eq.(11) to conveniently illustrate subsequent proofs of stability.

## B. Stability Analysis

**Lemma 1 (Jensen Inequality):** For a real convex function  $\varphi(\cdot)$ ,  $x_i, i \in [1, n]$  are in its domain, it can be derived that

$$\varphi\left(\frac{\sum_{i=1}^n x_i}{n}\right) \leq \frac{\sum_{i=1}^n \varphi(x_i)}{n} \quad (12)$$

**Lemma 2 (Quadratic Integral Inequality):** For a symmetric positive definite matrix  $R_{n \times n}$  and a differentiable  $n$ -dimension vector function  $\mathbf{x}(t) : [a, b] \rightarrow \mathbb{R}^n$ , it can be derived that

$$\int_a^b \dot{\mathbf{x}}(s)^T R \dot{\mathbf{x}}(s) ds \geq \frac{(\mathbf{x}(b) - \mathbf{x}(a))^T R (\mathbf{x}(b) - \mathbf{x}(a))}{b - a} \quad (13)$$

**Lemma 3 [35]:** Let  $\varphi_1, \varphi_2, \dots, \varphi_n : \mathbb{R}^m \rightarrow \mathbb{R}$  have positive values in an open subset  $S \in \mathbb{R}^m$ , it can be derived that

$$\begin{aligned} \min_{\{\alpha_i | \alpha_i > 0, \sum_i \alpha_i = 1\}} \sum_i \frac{1}{\alpha_i} \varphi_i(t) &= \sum_i \varphi_i(t) + \max_{g_{i,j}(t)} \sum_{i \neq j} g_{i,j}(t) \\ \text{s.t.} &\begin{cases} g_{i,j}(t) : \mathbb{R}^m \rightarrow \mathbb{R}, g_{i,j}(t) = g_{j,i}(t) \\ \begin{bmatrix} \varphi_i(t) & g_{i,j}(t) \\ g_{i,j}(t) & \varphi_j(t) \end{bmatrix} \geq 0 \end{cases} \end{aligned} \quad (14)$$

Some fundamental relationships are as follows.

$$\sum_{j=1}^n a_{ij} \leq n, \sum_{j=1}^n a_{ji} \leq n, \sum_{i=1}^n \sum_{j=1}^n a_{ij} b_j = \sum_{i=1}^n \sum_{j=1}^n a_{ij} b_i \quad (15)$$

The joint position error of the  $i$ -th robot is

$$\boldsymbol{\xi}_i = \mathbf{q}_i - \mathbf{q}_i^{\text{d}} \quad (16)$$

Taking the time derivative of Eq.(16) and substituting the control law Eq.(11) into  $\dot{\mathbf{q}}_i$  obtains

$$\dot{\boldsymbol{\xi}}_i = -\kappa \sum_{j=1}^n a_{ij} \boldsymbol{\xi}_i + \kappa \beta \sum_{j=1}^n a_{ij} \boldsymbol{\xi}_j(t - \tau_{ij}) \quad (17)$$

For the sake of brevity, the quadratic type  $\xi_i^T \kappa \xi_i$  is abbreviated as  $\kappa \xi_i^2$ .  $I_n$  denotes the n-dimensional identity matrix. Considering the following Lyapunov function

$$\begin{aligned} V(t) &= V_1 + V_2 + V_3 \\ V_1 &= \gamma_1 \sum_{i=1}^n \xi_i^2 \\ V_2 &= \gamma_2 \sum_{i=1}^n \sum_{j=1}^n a_{ji} \int_{t-\tau}^t \xi_i^2(s) ds \\ V_3 &= \gamma_3 \sum_{i=1}^n \sum_{j=1}^n a_{ji} \int_{-\tau}^0 \int_{t-\omega}^t \dot{\xi}_i^2(s) ds d\omega \end{aligned} \quad (18)$$

where  $\gamma_1, \gamma_2$  and  $\gamma_3$  are the positive coefficients of the Lyapunov function. Taking the time derivative of the Lyapunov function obtains

$$\begin{aligned} \dot{V}_1 &= \gamma_1 \sum_{i=1}^n 2\xi_i^T \dot{\xi}_i \\ \dot{V}_2 &= \gamma_2 \sum_{i=1}^n \sum_{j=1}^n a_{ji} (\xi_i^2 - \xi_i^2(t-\tau)) \\ \dot{V}_3 &= \gamma_3 \sum_{i=1}^n \sum_{j=1}^n a_{ji} (\tau \xi_i^2 - \int_{t-\tau}^t \dot{\xi}_i^2(s) ds) \end{aligned} \quad (19)$$

Then, each part of Eq.(19) is scaled. According to *Assumption 2*, substituting Eq.(17) into  $\dot{V}_1$  obtains

$$\begin{aligned} \dot{V}_1 &= -2\gamma_1 \kappa \sum_{i=1}^n \sum_{j=1}^n a_{ij} \xi_i^2 + 2\gamma_1 \kappa \beta \sum_{i=1}^n \sum_{j=1}^n a_{ij} \xi_i^T \xi_j(t-\tau_{ij}) \\ &\leq -2\gamma_1 \kappa \sum_{i=1}^n \xi_i^2 + 2\gamma_1 \beta \kappa \sum_{i=1}^n \sum_{j=1}^n a_{ij} \xi_i^T \xi_j(t-\tau_{ij}) \end{aligned} \quad (20)$$

According to the relationship Eq.(15), it can be obtained

$$\begin{aligned} \dot{V}_2 &= \gamma_2 \sum_{i=1}^n \sum_{j=1}^n a_{ji} \xi_i^2 - \gamma_2 \sum_{i=1}^n \sum_{j=1}^n a_{ji} \xi_i^2(t-\tau) \\ &\leq \gamma_2 \sum_{i=1}^n n \xi_i^2 - \gamma_2 \sum_{i=1}^n \sum_{j=1}^n a_{ji} \xi_i^2(t-\tau) \end{aligned} \quad (21)$$

$$\dot{V}_3 \leq \sum_{i=1}^n \gamma_3 n \tau \xi_i^2 - \sum_{i=1}^n \sum_{j=1}^n a_{ji} \gamma_3 \int_{t-\tau}^t \dot{\xi}_i^2(s) ds \quad (22)$$

By *Lemma 2*, it can be obtained

$$\begin{aligned} \int_{t-\tau}^t \dot{\xi}_i^2(s) ds &= \int_{t-\tau}^{t-\tau_{ji}} \dot{\xi}_i^2(s) ds + \int_{t-\tau_{ji}}^t \dot{\xi}_i^2(s) ds \\ &\geq \frac{(\xi_i(t-\tau_{ji}) - \xi_i(t-\tau))^2}{\tau - \tau_{ji}} + \frac{(\xi_i - \xi_i(t-\tau_{ji}))^2}{\tau_{ji}} \end{aligned} \quad (23)$$

By *Lemma 3*, the lower bound for convex combination of Eq.(23) is

$$\begin{aligned} \int_{t-\tau}^t \dot{\xi}_i^2(s) ds &\geq \frac{(\xi_i(t-\tau_{ji}) - \xi_i(t-\tau))^2}{\tau} \\ &\quad + \frac{(\xi_i - \xi_i(t-\tau_{ji}))^2}{\tau} \\ &\quad + \frac{(\xi_i(t-\tau_{ji}) - \xi_i(t-\tau))^T (\xi_i - \xi_i(t-\tau_{ji}))}{\tau} \\ &= \frac{1}{\tau} \left[ \xi_i^2(t-\tau_{ji}) + \xi_i^2(t-\tau) + \xi_i^2 - \xi_i^T \xi_i(t-\tau) \right. \\ &\quad \left. - \xi_i^T \xi_i(t-\tau_{ji}) - \xi_i^T(t-\tau_{ji}) \xi_i(t-\tau) \right] \\ &= \frac{1}{\tau} \left[ \frac{1}{2} \xi_i^2(t-\tau_{ji}) + \left( \frac{1}{2} \xi_i(t-\tau_{ji}) - \xi_i(t-\tau) \right)^2 \right. \\ &\quad \left. + \left( \frac{1}{2} \xi_i(t-\tau_{ji}) - \xi_i \right)^2 + \frac{1}{2} (\xi_i - \xi_i(t-\tau))^2 \right. \\ &\quad \left. - \frac{1}{2} \xi_i^2(t-\tau) - \frac{1}{2} \xi_i^2 \right] \\ &\geq \frac{1}{2\tau} \xi_i^2(t-\tau_{ji}) - \frac{1}{2\tau} \xi_i^2(t-\tau) - \frac{1}{2\tau} \xi_i^2 \end{aligned} \quad (24)$$

By using *Lemma 1* twice and Eq.(15), it can be obtained

$$\begin{aligned} \xi_i^2 &= \left[ -\kappa \sum_{j=1}^n a_{ij} \xi_i + \kappa \beta \sum_{j=1}^n a_{ij} \xi_j(t-\tau_{ij}) \right]^2 \\ &\leq 2 \left[ \sum_{j=1}^n a_{ij} \kappa \xi_i \right]^2 + 2\beta^2 \left[ \sum_{j=1}^n a_{ij} \kappa \xi_j(t-\tau_{ij}) \right]^2 \\ &\leq 2n \sum_{j=1}^n a_{ij} \kappa^2 \xi_i^2 + 2\beta^2 n \sum_{j=1}^n a_{ij} \kappa^2 \xi_j^2(t-\tau_{ij}) \end{aligned} \quad (25)$$

Substituting Eqs.(24)(25) into Eq.(22) and using Eq.(15) obtains

$$\begin{aligned} \dot{V}_3 &\leq \sum_{i=1}^n \gamma_3 n \tau \xi_i^2 - \sum_{i=1}^n \sum_{j=1}^n a_{ji} \gamma_3 \int_{t-\tau}^t \dot{\xi}_i^2(s) ds \\ &\leq 2\gamma_3 \tau n^2 \sum_{i=1}^n \sum_{j=1}^n a_{ij} \kappa^2 \xi_i^2 + \sum_{i=1}^n \sum_{j=1}^n a_{ji} \frac{\gamma_3}{2\tau} \xi_i^2(t-\tau) \\ &\quad + 2\gamma_3 \tau n^2 \beta^2 \sum_{i=1}^n \sum_{j=1}^n a_{ij} \kappa^2 \xi_j^2(t-\tau_{ij}) \\ &\quad - \sum_{i=1}^n \sum_{j=1}^n a_{ij} \frac{\gamma_3}{2\tau} \xi_j^2(t-\tau_{ij}) + \sum_{i=1}^n \frac{\gamma_3}{2\tau} n \xi_i^2 \\ &\leq \sum_{i=1}^n (2\gamma_3 \tau n^3 \kappa^2 + \frac{\gamma_3}{2\tau} n I_6) \xi_i^2 + \sum_{i=1}^n \sum_{j=1}^n a_{ji} \frac{\gamma_3}{2\tau} \xi_i^2(t-\tau) \\ &\quad + \sum_{i=1}^n \sum_{j=1}^n a_{ij} (2\gamma_3 \tau n^2 \beta^2 \kappa^2 - \frac{\gamma_3}{2\tau} I_6) \xi_j^2(t-\tau_{ij}) \end{aligned} \quad (26)$$

Integrating Eqs.(20)(21)(26) obtains

$$\begin{aligned} \dot{V} \leq & -\alpha_1 \sum_{i=1}^n \xi_i^2 - \alpha_2 \sum_{i=1}^n \sum_{j=1}^n a_{ij} \xi_j^2 (t - \tau_{ij}) \\ & - \alpha_3 \sum_{i=1}^n \sum_{j=1}^n a_{ji} \xi_i^2 (t - \tau) \end{aligned} \quad (27)$$

$$- \gamma_1 \beta \kappa \sum_{i=1}^n \sum_{j=1}^n a_{ij} \left( \xi_i - \frac{1}{2} \xi_j (t - \tau_{ij}) \right)^2$$

$$\begin{cases} \alpha_1 = 2\gamma_1 \kappa - 2\gamma_3 \tau n^3 \kappa^2 - \left( \gamma_2 + \frac{\gamma_3}{2\tau} + \gamma_1 \beta \kappa \right) n I_6 \\ \alpha_2 = \left( \frac{\gamma_3}{2\tau} - \gamma_1 \beta \kappa \right) I_6 - 2\gamma_3 \tau n^2 \beta^2 \kappa^2 \\ \alpha_3 = \left( \gamma_2 - \frac{\gamma_3}{2\tau} \right) I_6 \end{cases} \quad (28)$$

In order to ensure  $\dot{V} \leq 0$ ,  $\alpha_1$ ,  $\alpha_2$ , and  $\alpha_3$  must be semi-positive definite matrices, which denotes  $\alpha_1, \alpha_2, \alpha_3 > 0$  since they are diagonal matrices. For a system, the number of robots  $n$  and communication delay  $\tau$  are determined. The control law is designed by finding the coefficients  $k, \beta > 0$  such that there exists  $\gamma_1, \gamma_2, \gamma_3 > 0$  that satisfies  $\alpha_1, \alpha_2, \alpha_3 > 0$ . A simple design criterion is that the coefficients  $k, \beta$  are related to the communication delay. When the delay is large, the control coefficients should be smaller. Once the appropriate coefficients are found, it can be concluded that  $V \geq 0$  and  $\dot{V} \leq 0$ .  $\dot{V} = 0$  if and only if  $\xi_i = 0$  for  $i = 1, \dots, n$ . Thus, it can be deduced that the joint error  $\xi_i$  is asymptotically stable according to the Lyapunov theorem. In other words,  $\xi_i \rightarrow 0$  as  $t \rightarrow +\infty$ . Then,  $e_i^d - e_i \rightarrow 0$  and  $h_i - h_i^{\text{ref}} \rightarrow 0$ . By control law Eq.(9), the interaction wrench between robots and the object can be maintained at the desired target.

*Remark 1:* The control law does not correct the deviation of the planned trajectory. For example, if each robot has a pose deviation or velocity deviation, but the deviations are the same, then the input by Eq.(9) is zero since  $h_i = h_i^{\text{ref}}$  and  $h_j = h_j^{\text{ref}}$ . This is normal since only local information is used and thus cannot correct global errors.

*Remark 2:* The coefficients of Lyapunov function (18) are not specified and the conclusion Eqs.(28) may not seem very intuitive. However, if there is an accurate estimate of the object's stiffness and then  $K_0^{-1}K \approx I_6$ , the coefficients are relatively easy to find in practice because they are all linear inequalities.

### C. Simulations

In order to verify the stability of the control law, numerical simulations are performed on a computer with Intel Core i7-10700 CPU at 2.90 GHz (8 cores) and 64GB RAM. The results are obtained through Matlab 2022b. Consider a system of 5 robots manipulating objects on a 2D plane. Assuming that the ends of all robots move on the same 2D plane, and  $\dot{e}_i^{\text{ref}} = [0.1, 0.1]^T$  m/s,  $h_i^{\text{ref}} = [0, 0]^T$ ,  $i = 1, \dots, 5$ . The whole process is 60 seconds. Let  $\Omega(\cdot)$  denote a random number between -1 and 1. The stiffness of the object is assumed to be  $K = \text{diag}\{10.5, 9.5\}$ .

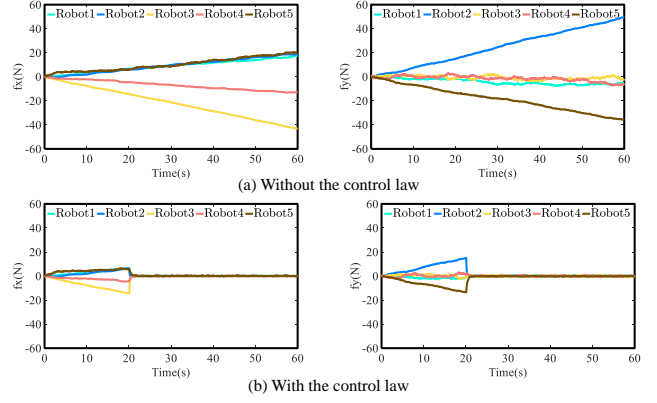


Fig. 2. The interaction wrenches between robots and the object. (a) Without the proposed control law. (b) With the proposed control law.

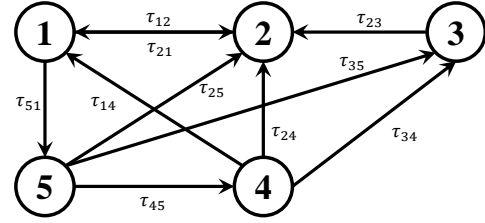


Fig. 3. The communication topology for multiple robots.

Due to some uncertainties and the deviation between the planned robot model and the actual robot model, it is impossible to achieve the planned velocity. The actual end velocities of robots are shown in Table I. If the deviation is not corrected by employing the control law, it will result in increased interaction wrenches, as illustrated in Fig. 2(a). In the simulation, two types of errors are introduced. One type is random velocity error, and the other is velocity bias. The bias can be caused by the relative pose errors of the robots. Both types of errors are very common in practice, and may cause increased interaction wrenches.

The proposed control law Eq.(9) is verified by enrolling it after 20s in the process described above. The communication topology is shown in Fig. 3. As described before, time delays are non-uniform, asymmetric, and time-varying, and they are assumed to be  $\tau_{12} = 0.01|\sin(t)|$ ,  $\tau_{14} = 0.01|\cos(t)|$ ,  $\tau_{21} = 0.02/t$ ,  $\tau_{23} = 0.02/t^2$ ,  $\tau_{24} = e^{-t}$ ,  $\tau_{25} = t/e^t$ ,  $\tau_{34} = 0.004\ln(t)$ ,  $\tau_{35} = 0.02/\ln(t)$ ,  $\tau_{45} = 0.01|\Omega(t)|$ ,  $\tau_{51} = 0.01|\Omega(t)|$ . The control coefficients are set as  $K_0 = \text{diag}\{10, 10\}$  and  $k = 0.5, \beta = 0.1$ . According to these time delays and  $t \in [20, 60]$ , the bound  $\tau$  is 0.01s. These parameters

TABLE I  
THE ACTUAL END VELOCITY (M/S) OF EACH ROBOT

$\dot{e}_1$	$[0.1 + 0.05\Omega(t), 0.1 + 0.1\Omega(t)]^T$
$\dot{e}_2$	$[0.1 + 0.01\sin(t), 0.08]^T$
$\dot{e}_3$	$[0.12, 0.1 + 0.2\Omega(t)]^T$
$\dot{e}_4$	$[0.11 + 0.05\Omega(t)\sin(t), 0.1 + 0.2\Omega(t)]^T$
$\dot{e}_5$	$[0.1 + 0.1\Omega(t), 0.11]^T$

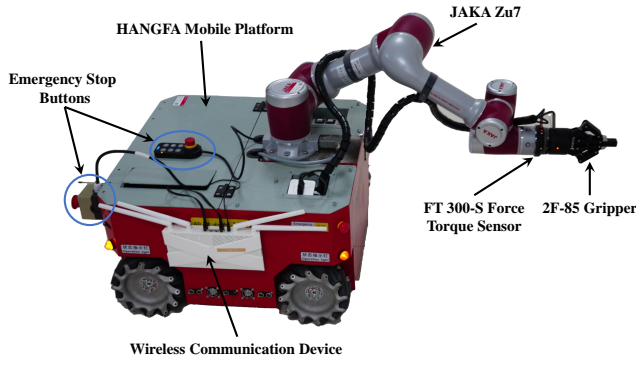


Fig. 4. The physical model of a mobile manipulator robot used in experiments. The robot consists of an omnidirectional wheeled platform and a 6-DOF manipulator. A force sensor and a gripper are equipped at the end of the robot for manipulating objects. A router is attached for communication between different robots.

substituted into Eq.(28) satisfy  $\alpha_1, \alpha_2, \alpha_3 > 0$ . Therefore, the control law Eq.(9) is stable. The results are illustrated in Fig. 2(b). After 20 seconds, the control law is enrolled, and the force data is quickly adjusted to the desired value. Although we use five robots as an example, the control law can easily be extended to more robots. The computation of the control law Eq.(9) itself is not complex.

#### IV. EXPERIMENTS AND DISCUSSIONS

##### A. Experimental Setup

The proposed control law is verified in physical experiments. Each robot is composed of a HANGFA omnidirectional wheeled platform and a JAKA Zu7 manipulator. The end of each manipulator is equipped with a Robotiq FT 300-S Force Torque Sensor and a Robotiq 2F-85 Gripper. These devices and the robot are controlled by its onboard Next Unit of Computing (NUC) computer with Intel Core i7-1165G7 CPU at 2.80 GHz (4 cores) and 16GB RAM. The control frequency of the robots is 25 Hz. Besides, each robot is equipped with wireless transmission modules in the same local network for communication. The communication framework is implemented and achieved through ROS-melodic. Generally, the communication delays are less than 0.01s. The physical robot is shown in Fig. 4. The forward and inverse kinematics of the robot are based on our previous work [36].

##### B. Experimental Results

The control law is validated through experiments involving two robots cooperating to manipulate objects. In the first experiment, the robots collaborate to perform reciprocating rotational motions with an acrylic sheet, and the oscillation angle ranges from -15 to 15 degrees. The sheet measures 1m in length, 0.4m in width, and 0.003m in thickness, with a weight of 14N. The expected interaction wrenches of robots in the world frame are  $\mathbf{h}_1^{\text{ref}} = [\mathbf{f}_1^{\text{ref}}, \mathbf{t}_1^{\text{ref}}]^T$ ,  $\mathbf{f}_1^{\text{ref}} = [10, 0, -7]^T N$ ,  $\mathbf{t}_1^{\text{ref}} = [0, 0, 0]^T Nm$ ,  $\mathbf{f}_2^{\text{ref}} = [-10, 0, -7]^T N$ ,  $\mathbf{t}_2^{\text{ref}} = [0, 0, 0]^T Nm$ . The weight is evenly distributed in the  $z$ -direction by two robots, and a 10N force in the

$x$ -direction is applied to maintain the stability of the object. The coefficients in the control law Eq.(9) are set as  $K_0 = \text{diag} \{5 \times 10^5, 2 \times 10^5, 2 \times 10^5, 10^2, 10^2, 10^2\}$  and  $k = 0.5, \beta = 0.2$ .

The process of the experiment is illustrated in Fig. 5, and the motion duration is 83.2 seconds. The experiment is repeated twice, once without the control law and once with. The results of interaction wrenches are shown in Fig. 6. Without the control law, the interaction wrenches could not be maintained at the desired values. Especially in the  $x$ -direction, the forces are very large due to the pushing and pulling between the robots when cooperatively manipulating the object. Additionally, in the  $z$ -direction, the robots could not evenly share the load. These increased interaction wrenches do not contribute to supporting or manipulating the object, instead, they may cause damage to both the object and the robots. In contrast, with the control law applied, the interaction wrenches are maintained at the desired values in all six directions. Compared to the scenario without the control law, implementing the control law reduces the maximum error by [93.37, 66.62, 92.38, 68.75, 58.82, 64.24]% and the average error by [98.68, 93.49, 96.58, 55.36, 61.96, 84.89]% for robot1 in the corresponding directions, and the maximum error by [94.38, 72.55, 93.30, 75.74, 70.18, 26.05]% and the average error by [98.56, 90.15, 97.30, 74.94, 73.36, 37.10]% for robot2 in the corresponding directions. The total wrenches on the object are shown in Fig. 7. It can be seen that after applying the control law, the fluctuation range of the total wrenches on the object is also relatively smaller.

In the second experiment, the robots cooperatively transport an object to a desired location. The object is an aluminum frame, weighing 10N. The entire motion of robots is planned in advance, with the expected interaction wrenches  $\mathbf{f}_1^{\text{ref}} = [10, 0, -5]^T N$ ,  $\mathbf{t}_1^{\text{ref}} = [0, 0, 0]^T Nm$ ,  $\mathbf{f}_2^{\text{ref}} = [-10, 0, -5]^T N$ ,  $\mathbf{t}_2^{\text{ref}} = [0, 0, 0]^T Nm$ . The coefficients in the control law Eq.(9) are set as  $K_0 = \text{diag} \{10^6, 10^5, 10^5, 10^2, 10^2, 10^2\}$  and  $k = 0.5, \beta = 0.2$ .

The process of the experiment is illustrated in Fig. 8, and the motion duration is 130.4 seconds. From 17s to 57s, the platforms move forward simultaneously to avoid exceeding the reachable space of the manipulators. From 70s to 100s, the platforms move laterally simultaneously to transport the object. As shown in Fig. 9, it can be seen that without the control law, the interaction wrenches vary greatly, especially in the  $f_x$  directions. Compared to the scenario without the control law, implementing the control law reduces the maximum error by [45.97, 54.18, 53.56, 81.85, 77.39, 21.52]% and the average error by [85.92, 62.72, 60.49, 93.13, 88.80, 67.99]% for robot1 in the corresponding directions, and the maximum error by [45.47, 34.97, 52.53, 73.38, 74.41, 46.05]% and the average error by [86.38, 58.44, 69.38, 85.51, 83.32, 72.44]% for robot2 in the corresponding directions.

When only the manipulators are moving, the interaction wrenches are well maintained. However, when the mobile platforms are moving (from 17s to 57s and from 70s to 100s), the force oscillation range becomes significantly larger. Additionally, some impacts occur due to the starting and stopping of the mobile platform. From this, it is evident that



Fig. 5. Two mobile manipulator robots cooperatively manipulate an object to perform a reciprocating rotational motion, with the object's angle ranging between  $-15$  degrees and  $15$  degrees.

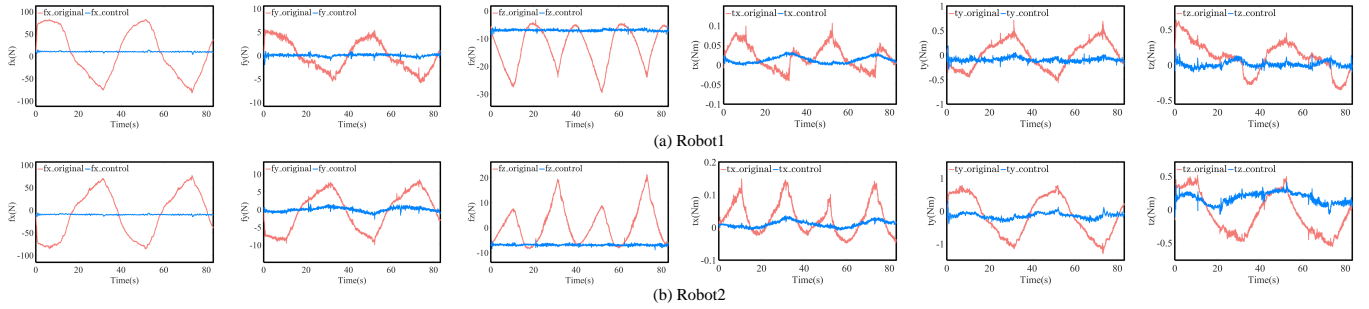


Fig. 6. Comparison between applying and not applying the control law. The interaction wrenches in the world frame without (with) applying the control law is represented by the red (blue) curve. The desired interaction wrenches are  $[10, 0, -7, 0, 0, 0]^T$  for robot1 and  $[-10, 0, -7, 0, 0, 0]^T$  for robot2.

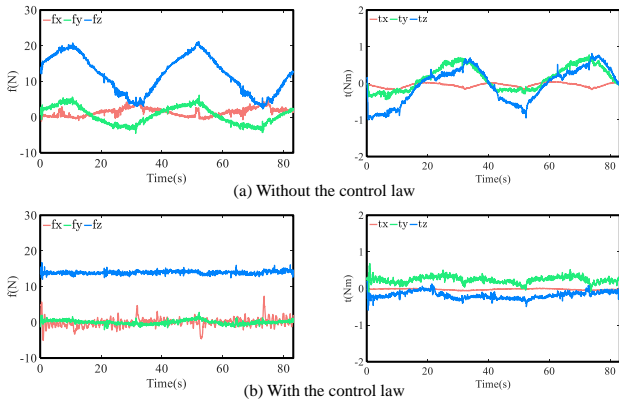


Fig. 7. The total wrenches applied to the object during cooperation manipulation by multiple mobile manipulator robots.

the accuracy of the manipulator is much higher than that of the omnidirectional wheel. Therefore, the control law is designed utilizing the motion of manipulators to correct errors.

### C. Discussion and Limitation

The stability of the proposed control law has been proven, and subsequent simulations and experiments have demonstrated that the proposed control law effectively maintains the desired interaction wrenches. Due to positioning errors or control errors, the theoretical planned motion cannot achieve desired cooperative performance, and the errors will result in increased internal wrenches. Reducing unnecessary interaction wrenches is essential for ensuring the safety of both the object and the robots, and reducing emergency stops during collaborative manipulation. Compared to other control

methods, the proposed control law only utilizes local force sensor information, eliminating the need for a large range of accurate positioning devices. Therefore, it is more suitable for real-world applications. Additionally, the communication delay between robots are considered, and it has been proven that the control law is robust against delays.

However, the proposed control strategy also has some limitations. First, the stiffness of the object is required. This parameter often requires empirical values or preliminary experimental determination. Improper setting may lead to instability or divergence of the control law. Second, the effect of acceleration is not considered in Eq.(8) The control law is only suitable for quasi-static processes, so the impact in the experiment cannot be corrected, as shown in Fig. 9. Finally, the motion of the mobile platform has not been taken into account to correct errors, which could lead to failure if the error becomes too large and exceeds the reachable space of the manipulators.

## V. CONCLUSION AND FUTURE WORK

This paper aims to reduce the interaction wrenches during the cooperative manipulation of multiple mobile manipulator robots. A distributed motion control law is proposed. Since the manipulator is more accurate than the mobile platform, the control law only operates on the manipulators. The control law is proven to be stable under certain conditions. Then, the control law is verified in real-world experiments. Experimental results, involving the cooperative manipulation of two robots transporting an object, effectively validate the effectiveness of the proposed control law. It is shown that the proposed control law is convenient to be applied in real-world applications as it does not rely on global position and velocity information.

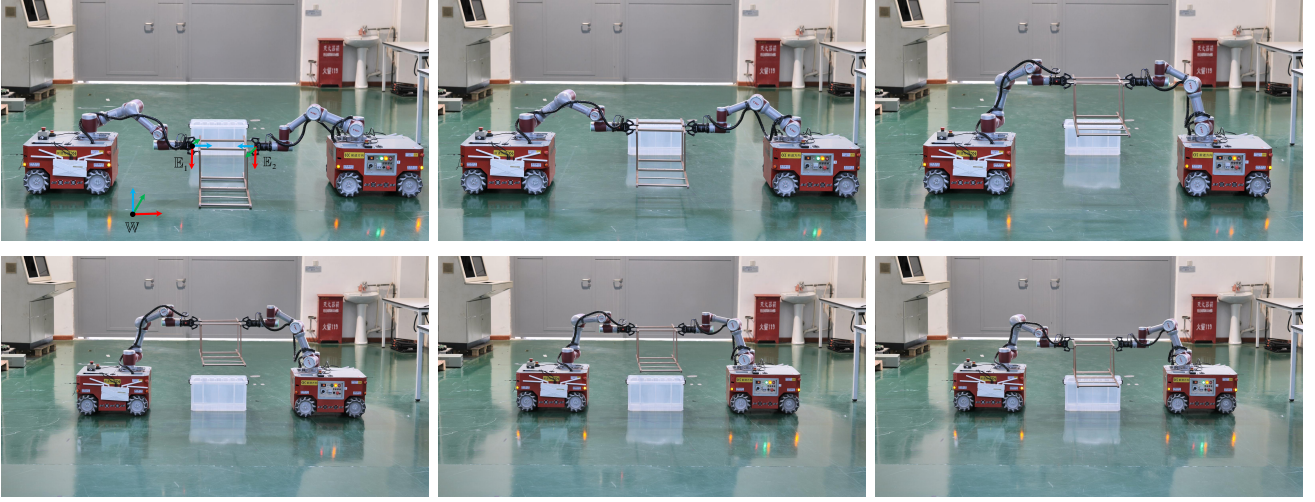


Fig. 8. Two mobile manipulator robots cooperatively transport an object. They first lift the object, then move it to the target position, and finally put it down.

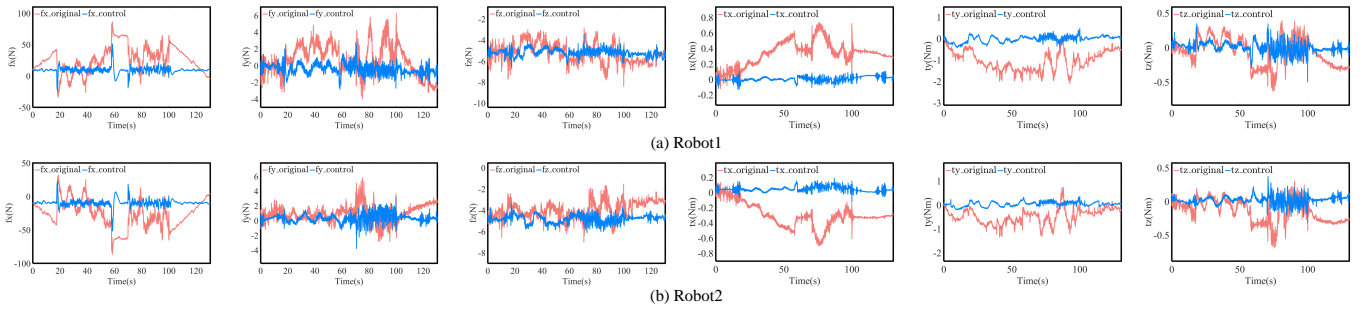


Fig. 9. Comparison between applying and not applying the control law. The force sensor data without (with) applying the control law is represented by the red (blue) curve. The desired interaction wrenches are  $[10, 0, -5, 0, 0, 0]^T$  for robot1 and  $[-10, 0, -5, 0, 0, 0]^T$  for robot2.

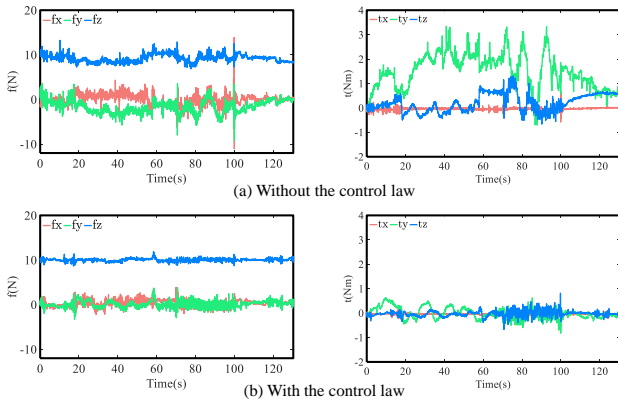


Fig. 10. The total force applied to the object during cooperation manipulation by multiple mobile manipulator robots.

Regarding future work, on the one hand, we will further refine the control strategy. The dynamics model of the robot will be considered to reduce impact forces when the robot's velocity changes. On the other hand, more complex manipulation tasks and manipulating heavier objects will be considered. We will strive to further enhance the control method through real-world manipulation tasks.

## REFERENCES

- [1] S. Thakar, P. Rajendran, A. M. Kabir, and S. K. Gupta, "Manipulator motion planning for part pickup and transport operations from a moving base," *IEEE Trans. Automat. Sci. Eng.*, vol. 19, no. 1, pp. 191–206, 2020.
- [2] K. Jang, S. Kim, and J. Park, "Motion planning of mobile manipulator for navigation including door traversal," *IEEE Robot. Automat. Lett.*, 2023.
- [3] B. Tao, X. Zhao, and H. Ding, "Mobile-robotic machining for large complex components: A review study," *Sci. China-Technol. Sci.*, vol. 62, pp. 1388–1400, 2019.
- [4] M. Dogar, R. A. Knepper, A. Spielberg, C. Choi, H. I. Christensen, and D. Rus, "Multi-scale assembly with robot teams," *Int. J. Robot. Res.*, vol. 34, no. 13, pp. 1645–1659, 2015.
- [5] B. Tao, Z. Gong, and H. Ding, "Robotic cluster machining: Manufacturing revolution for large and complex components," pp. 2215–2217, 2022.
- [6] Z. Feng, G. Hu, Y. Sun, and J. Soon, "An overview of collaborative robotic manipulation in multi-robot systems," *Ann. Rev. Contr.*, vol. 49, pp. 113–127, 2020.
- [7] Y. Cui, Z. Xu, L. Zhong, P. Xu, Y. Shen, and Q. Tang, "A task-adaptive deep reinforcement learning framework for dual-arm robot manipulation," *IEEE Trans. Automat. Sci. Eng.*, 2024.
- [8] D. Sieber and S. Hirche, "Human-guided multirobot cooperative manipulation," *IEEE Trans. Contr. Syst. Technol.*, vol. 27, no. 4, pp. 1492–1509, 2018.
- [9] A. Marino, "Distributed adaptive control of networked cooperative mobile manipulators," *IEEE Trans. Contr. Syst. Technol.*, vol. 26, no. 5, pp. 1646–1660, 2017.
- [10] T. G. Sugar and V. Kumar, "Control of cooperating mobile manipulators," *IEEE Trans. Robot. Automat.*, vol. 18, no. 1, pp. 94–103, 2002.
- [11] Z. Zhang, J. Mao, H. Tan, Y. Jiang, Y. Feng, Y. Wu, and Y. Wang, "Hybrid force/position control of multi-mobile manipulators for cooperative

- operation without force measurements,” *IEEE Trans. Circuits Syst. I*, vol. 71, no. 1, pp. 397–410, 2023.
- [12] C. Wu, H. Fang, Q. Yang, X. Zeng, Y. Wei, and J. Chen, “Distributed cooperative control of redundant mobile manipulators with safety constraints,” *IEEE Trans. Cybernetics*, vol. 53, no. 2, pp. 1195–1207, 2021.
- [13] J. Alonso-Mora, S. Baker, and D. Rus, “Multi-robot formation control and object transport in dynamic environments via constrained optimization,” *Int. J. Robot. Res.*, vol. 36, no. 9, pp. 1000–1021, 2017.
- [14] Z. Li, P. Y. Tao, S. S. Ge, M. Adams, and W. S. Wijesoma, “Robust adaptive control of cooperating mobile manipulators with relative motion,” *IEEE Trans. Syst., Man, Cybern., Cybern.*, vol. 39, no. 1, pp. 103–116, 2008.
- [15] V. Andaluz, V. Rampinelli, F. Roberti, and R. Carelli, “Coordinated cooperative control of mobile manipulators,” in *Proc. IEEE Int. Conf. Ind. Technol.* IEEE, 2011, pp. 300–305.
- [16] C. P. Bechlioulis and K. J. Kyriakopoulos, “Collaborative multi-robot transportation in obstacle-cluttered environments via implicit communication,” *Front. Robot. AI*, vol. 5, p. 90, 2018.
- [17] J. Chen and S. Kai, “Cooperative transportation control of multiple mobile manipulators through distributed optimization,” *Sci. China-Inf. Sci.*, vol. 61, no. 12, p. 120201, 2018.
- [18] Y. Kume, Y. Hirata, and K. Kosuge, “Coordinated motion control of multiple mobile manipulators handling a single object without using force/torque sensors,” in *Proc. IEEE/RSJ Int. Conf. Intell. Robot. Syst.* IEEE, 2007, pp. 4077–4082.
- [19] Z. Wang and M. Schwager, “Kinematic multi-robot manipulation with no communication using force feedback,” in *Proc. IEEE Int. Conf. Robot. Autom.* IEEE, 2016, pp. 427–432.
- [20] —, “Force-amplifying n-robot transport system (force-ants) for cooperative planar manipulation without communication,” *Int. J. Robot. Res.*, vol. 35, no. 13, pp. 1564–1586, 2016.
- [21] Y. Ren, S. Sosnowski, and S. Hirche, “Fully distributed cooperation for networked uncertain mobile manipulators,” *IEEE Trans. Robotics*, vol. 36, no. 4, pp. 984–1003, 2020.
- [22] D. Qin, J. Wu, A. Liu, W.-A. Zhang, and L. Yu, “Cooperation and coordination transportation for nonholonomic mobile manipulators: A distributed model predictive control approach,” *IEEE Trans. Syst., Man, Cybern., Syst.*, vol. 53, no. 2, pp. 848–860, 2022.
- [23] A.-N. Ponce-Hinestroza, J.-A. Castro-Castro, H.-I. Guerrero-Reyes, V. Parra-Vega, and E. Olguín-Díaz, “Cooperative redundant omnidirectional mobile manipulators: Model-free decentralized integral sliding modes and passive velocity fields,” in *Proc. IEEE Int. Conf. Robot. Autom.* IEEE, 2016, pp. 2375–2380.
- [24] G.-B. Dai and Y.-C. Liu, “Distributed coordination and cooperation control for networked mobile manipulators,” *IEEE Trans. Ind. Electron.*, vol. 64, no. 6, pp. 5065–5074, 2016.
- [25] C. K. Verginis, M. Mastellaro, and D. V. Dimarogonas, “Robust cooperative manipulation without force/torque measurements: Control design and experiments,” *IEEE Trans. Contr. Syst. Technol.*, vol. 28, no. 3, pp. 713–729, 2019.
- [26] P. Xu, Y. Cui, Y. Shen, W. Zhu, Y. Zhang, B. Wang, and Q. Tang, “Reinforcement learning compensated coordination control of multiple mobile manipulators for tight cooperation,” *Eng. Appl. Artif. Intell.*, vol. 123, p. 106281, 2023.
- [27] Z. Li, C. Yang, C.-Y. Su, S. Deng, F. Sun, and W. Zhang, “Decentralized fuzzy control of multiple cooperating robotic manipulators with impedance interaction,” *IEEE Trans. Fuzzy Syst.*, vol. 23, no. 4, pp. 1044–1056, 2014.
- [28] X. Zhou, G. Zhao, Y. Xing, J. Wu, and Z. Xiong, “Robotic stacking of irregular objects with load position identification and compensation,” in *Proc. IEEE Conf. Automat. Sci. Eng.*, 2023, pp. 1–7.
- [29] S. Erhart and S. Hirche, “Model and analysis of the interaction dynamics in cooperative manipulation tasks,” *IEEE Trans. Robotics*, vol. 32, no. 3, pp. 672–683, 2016.
- [30] —, “Internal force analysis and load distribution for cooperative multi-robot manipulation,” *IEEE Trans. Robotics*, vol. 31, no. 5, pp. 1238–1243, 2015.
- [31] T. Xu, T. Yang, Z. Duan, G. Feng, and G. Chen, “Distributed coordination of networked manipulators: A two-layer control scheme,” *IEEE Trans. Contr. Syst. Technol.*, vol. 31, no. 6, pp. 2660–2672, 2023.
- [32] C. K. Verginis, D. Zelazo, and D. V. Dimarogonas, “Cooperative manipulation via internal force regulation: A rigidity theory perspective,” *IEEE Transactions on Control of Network Systems*, 2022.
- [33] N. E. Carey and J. Werfel, “Collective transport of unconstrained objects via implicit coordination and adaptive compliance,” in *2021 IEEE International Conference on Robotics and Automation (ICRA)*. IEEE, 2021, pp. 12 603–12 609.
- [34] K. Yamazaki, S. Suzuki, and Y. Kuribayashi, “Approaching motion planning for mobile manipulators considering the uncertainty of self-positioning and object’s pose estimation,” *Robot. Auton. Syst.*, vol. 158, p. 104232, 2022.
- [35] P. Park, J. W. Ko, and C. Jeong, “Reciprocally convex approach to stability of systems with time-varying delays,” *Automatica*, vol. 47, no. 1, pp. 235–238, 2011.
- [36] H. Zhang, Q. Sheng, J. Hu, X. Sheng, Z. Xiong, and X. Zhu, “Cooperative transportation with mobile manipulator: A capability map-based framework for physical human–robot collaboration,” *IEEE/ASME Trans. Mechatronics*, vol. 27, no. 6, pp. 4396–4405, 2022.